UDC 517.9

RATIONAL SPECTRAL COLLOCATION COMBINED WITH THE SINGULARITY SEPARATED METHOD FOR SECOND-ORDER SINGULAR PERTURBATION PROBLEMS*

РАЦІОНАЛЬНА СПЕКТРАЛЬНА КОЛОКАЦІЯ, ОБ'ЄДНАНА З МЕТОДОМ ВІДОКРЕМЛЕННЯ ОСОБЛИВОСТІ ДЛЯ СИНГУЛЯРНИХ ПРОБЛЕМ ЗБУРЕННЯ ДРУГОГО РОДУ

Y. Lufeng

School Math. and Statist., Lanzhou Univ., Lanzhou, 730000, China,
School Math. and Inform. Sci., North Minzu Univ., Yinchuan, 750021, China
e-mail: ylf-sd@163.com

W. Yujiang

School Math. and Statist., Lanzhou Univ., Lanzhou, 730000, China
e-mail: myjaw@lzu.edu.cn

Novel rational spectral collocation is presented combined with the singularity-separated method for second-order singularly perturbed boundary-value problems. The solution is presented in the form $u = w + v$, where w is the solution of the corresponding third boundary-value problem and v is a singular function with explicit expression. The auxiliary third boundary-value problem is solved by the rational spectral collocation method combined with asymptotic theory (RSCAT). According to asymptotic analysis, the parameters of the $\sinh$-transformation can be determined by the location and width of the boundary layers. The parameters in the singular correction can be determined by the boundary conditions of the original problem. Numerical experiments are carried out to demonstrate the computational efficiency and accuracy of our method.

Наведено нову раціональну спектральну колокацію, об'єднану з методом відокремлення особливості для сингулярно збуреної крайової задачі другого роду. Розв'язок подано у вигляді $u = w + v$, де w — розв'язок відповідної третьої крайової задачі, а v — сингулярна функція у явному вигляді. Допоміжну третю крайову задачу розв'язано за допомогою раціонального методу спектральної колокації з урахуванням асимптотичної теорії. Згідно з асимптотичним аналізом параметри $\sinh$-перетворення визначаються розташуванням і шириною примежових шарів. Параметри сингулярної поправки знаходяться з граничних умов вихідної задачі. Результати виконаних числових експериментів демонструють обчислювальну ефективність і точність запропонованого методу.

1. Introduction. Singular perturbation problems, such as fluid mechanics boundary layers, quantum mechanics transition points and flow under large Reynolds number, arise in the mathematical modeling of physical and engineering problems. Over the past few decades, singular perturbation has received extensive attention. Singular perturbation boundary value problems have

The work is partially supported by the Research Project of Science and Technology of Colleges and Universities in Ningxia (No. NGY2020056), First-Class Disciplines Foundation of Ningxia (No. NXYLXK2017B09) and High-level achievements climbing project of first-class mathematics discipline (No. sxylxk202137).

© Y. Lufeng, W. Yujiang, 2021

either boundary layers or internal layers where the solution drastically changes. Detailed theories and analysis of the singular perturbation problem can be found in the literature [1 – 3]. These problems have steep gradients in the narrow layers within the considered region, wherein the dependent variable undergoes rapid changes; therefore, the traditional numerical method is not suitable for solving singular perturbation problems, as the grid is not fine enough to describe the internal rules in these layers. To distinguish these regions, a finer mesh is needed to increase the number of computations. Therefore, special methods are required to obtain good numerical approximations to such problems.

Some conventional asymptotic methods can be used to approximate solutions for singular perturbation problems. Asymptotic methods decompose the area into the boundary layer (where the solution exhibits rapid change) and the outer region (which is far from the inner region) [4]. At the boundary layer, a scaling transformation is introduced to amplify the boundary layer region. Then, an internal solution (in the form of a series) is obtained. The solution of the reduced problem is approximated in exponential form at the outer region. Finally, these two approximations are matched to obtain a uniformly valid approximation using the limit process. Some asymptotic methods are the Method of Matched Asymptotic Expansions (MMAE) [5], the Method of Multiple-scale Analysis, the Periodic Averaging Method and the Method of Wentzel – Kramers – Brillouin (WKB) Approximation [6, 7]. He matching procedure may be onerous or impossible.

Additionally, several numerical methods have been developed to solve singular perturbation problems. To address severely oscillating defects on the boundary layer, Shishkin's mesh grid was proposed to construct uniform grids on the outer and inner regions [8]. The results of Shishkin's method in terms of convergence, stability and error estimation can be found in Madden [9], Lin β [10]. The cubic spline method and uniform convergence difference scheme on a uniform grid were constructed to solve second-order singular perturbation problems [11].

The spectral collocation method based on rational interpolation in barycentric form (RCM) was proposed by Berrut and his collaborators [12, 13]. With RCM, the first- and second-order differentiation matrices are given by the barycentric weights and interpolation points. In addition, a $\sinh$-transform maps the Chebyshev points clustered near the boundaries of $[-1, 1]$ into a new set of collocation points (i.e., more points are present in the boundary layers). The parameters of the $\sinh$-transform are determined by the width and position of the boundary layer. Chen and Wang [14, 15] applied a rational spectral collocation in barycentric form with $\sinh$-transform to solve a coupled system of singularly perturbed problems and third-order singularly perturbed problems.

To weaken the singularity and improve the accuracy of numerical simulation, the singularity-separated technique (SST) for singular perturbation problems with constant coefficients was proposed by Chen and Yang [16], and finite element methods with SST were used to solve singular perturbation problems with a single boundary layer.

In this paper, we consider the following one-dimensional singular perturbation problem

$$\begin{cases} Au := -\varepsilon u'' + b(x)u' + c(x)u = f, \quad x \in \Omega = (0,1), \\ u(0) = \alpha, \quad u(1) = \beta, \end{cases} \tag{1.1}$$

where ε is the perturbation parameter, constants $c \geq 0$. The solution has the singularity in the

boundary layer near $x = 1$ when $b > 0$. When $b = 0$, the solution to the problem of this type has two boundary layers with width $O(\sqrt{\varepsilon})$ at $x = 0$ and $x = 1$, respectively. The smaller ε is, the thinner the boundary layer is.

Here, we present a novel numerical method based on rational spectral collocation in barycentric form with the singularly separated method (RSC-SSM) to solve second-order singularly perturbed boundary-value problems in various fields.

This paper is organized as follows. An overview of asymptotic analysis and the $\sinh$-transform are outlined in Section 2. The algorithmic details of RSC-SSM for second-order singularly perturbed boundary-value problems are provided in Section 3. Section 4 presents numerical results for two test problems, which demonstrate that the new schemes lead to large performance gains over RSCAT in the literature. Finally, we present some Conclusions in Section 5.

1.1. Asymptotic expansion approximation.

Lemma 1. *If $b > 0$, the solution of (1.1) could be expressed as follows:*

$$u(x) = w(x) + v(\xi) + O(\varepsilon), \quad \xi = \frac{1-x}{\varepsilon}. \tag{1.2}$$

where $\omega(x)$ and $v(\xi)$ is the solution of following equations, respectively:

$$\begin{cases} bw' + cw = f(x), & 0 < x < 1, \\ w(0) = \alpha, \end{cases} \tag{1.3}$$

and

$$\begin{cases} v'' + bv' = 0, & \xi > 0, \\ v(1) = \beta - w(1), & v'(1) = -b(\beta - w(1)). \end{cases} \tag{1.4}$$

Proof. Let $w(x)$ be the solution of the reduced problem (1.3), $v(\xi)$ is the solution of the boundary layer correction problem,

$$\begin{cases} v'' + bv' = 0, & \xi > 0, \\ v(1) = \beta - w(1), & \lim\limits_{\xi\to\infty} v(\xi) = 0. \end{cases} \tag{1.5}$$

We rewrite Eq. (1.5):

$$\begin{cases} v'' + bv' = 0, & \xi > 0, \\ v(1) = \beta - w(1), & v'(1) = \gamma. \end{cases} \tag{1.6}$$

where γ is determined by $\lim_{\xi\to\infty} v(\xi) = 0$.

Integrating Eq. (1.6) once gives

$$v'(\xi) = \gamma e^{b} e^{-b\xi}.$$

Integrating again yields

$$v(\xi) = -\frac{\gamma}{b}\, e^{b(1-\xi)} + \beta - w(1) + \frac{\gamma}{b}.$$

By $v(\infty) = 0$, we get

$$\gamma = -b(\beta - w(1)).$$

Theorem 1 [17]. *If $b > 0$, the solution of (1.1) has the following asymptotic expansion:*

$$u(x) = w(x) + \bar{v}_0(\xi) + O(\varepsilon),$$

where

$$\bar{v}_0(\xi) = \begin{cases} v_0(\xi), & 0 \le \xi \le T, \\ 0, & \xi > T, \end{cases} \qquad T = \frac{1}{b(1)} \ln \frac{\varepsilon}{|\beta - w(1)|}, \tag{1.7}$$

satisfying the inequality

$$\|u(x) - (w(x) + \bar{v}_0(\xi))\| \le C\varepsilon,$$

where C is a generic constant.

The above theorem suggests that the boundary layer of the convection-diffusion problem $(b > 0)$ is located at the right endpoint of the underlying interval $[0, 1]$ and its width is $\delta = T\varepsilon$.

A similar conclusion can be drawn for the reaction diffusion equation $(b = 0)$.

Theorem 2. *If $b = 0$, the solution of (1.1) has the asymptotic expansion*

$$u(x) = w(x) + \bar{v}(x) + O(\sqrt{\varepsilon}),$$

where

$$\bar{v}(x) = \begin{cases} v(x), & x \in [0, \tau_0] \cup [1 - \tau_0, 1], \\ 0, & x \in [\tau_0, 1 - \tau_0], \end{cases} \qquad 0 < \tau_0 = -\frac{\sqrt{\varepsilon}}{\alpha} \ln \sqrt{\varepsilon} \ll 1, \tag{1.8}$$

satisfying the inequality

$$\|u(x) - (w(x) + \bar{v}_0(x))\| \le C\sqrt{\varepsilon},$$

where C is a generic constant.

The Theorem 2 suggests that the boundary layers of the reaction-diffusion problem are located at the two endpoints of the underlying interval $[0, 1]$ and their width is $\delta = \tau_0$.

1.2. Rational spectral collocation method in barycentric form. Rational function $p_N(x)$ in barycentric form, which interpolates function $u(x)$ at $N + 1$ distinct points $\{x_k\}_{k=0}^N$ can be expressed as [18]

$$u(x) \approx p_N(x) = \frac{\sum_{k=0}^N \dfrac{\omega_k}{x - x_k} u(x_k)}{\sum_{k=0}^N \dfrac{\omega_k}{x - x_k}} \tag{1.9}$$

where $\{\omega_k\}_{k=0}^N$ are barycentric weights. Most important in practice are the so-called Chebyshev – Gauss – Lobatto (CGL) points

$$x_k = -\cos(k\pi/N),$$

which leading to so-called simplified weights are chosen as [18],

$$\omega_0 = \frac{1}{2}, \quad \omega_k = (-1)^k, \quad k = 1, 2, \ldots, N - 1, \quad \omega_N = \frac{(-1)^N}{2}.$$

The rational interpolation based on the barycentric form with transformed Chebyshev points has the following convergence analysis.

Theorem 3 [19]. *Let $D_1,\ D_2$ be two domains of C containing $J=[-1,1]$ and real interval I, respectively. Let $g\colon D_1\to D_2$ be a conformal map, such that $g(J)=I$, and $u\colon D_2\to C$ such that the composition $u\circ g\colon D_1\to C$ is analytic inside and on an ellipse $C_\rho(\subset D_1)$, with foci at ±1 and with the sum of its major and minor axes equal to $\rho>1$. Let $p_N(x)$ be the rational interpolation of u between the transformed Chebyshev points $\hat{x}_k:=g(-cos(k\pi/N))$. Then,*

$$\forall x\in[-1,1]\quad \|p_N(x)-u(x)\|=O\left(\rho^{-N}\right).$$

The nth order derivatives of p_N can be determined the nth order differentiation matrix $\left\{D_{jk}^{(n)})\right\}_{j,k=0}^{N}$ associated with p_N represented by (1.9) at the point x_j:

$$p_N^{(n)}(x_j)=\sum_{k=0}^{N}\frac{d^n}{dx^n}\left(\frac{\dfrac{\omega_k}{x-x_k}u(x_k)}{\sum_{l=0}^{N}\dfrac{\omega_l}{x-x_l}}\right)_{x=x_j}=\sum_{k=0}^{N}D_{jk}^{(n)}u(x_k),\quad j=0,1,\dots,N,$$

where the entries of 1st and nth differentiation matrices are given as follow [18]:

$$D_{jk}^{(1)}=\begin{cases}\dfrac{\omega_k}{\omega_j}\,(x_j-x_k), & j\neq k,\\ -\sum_{i\neq k}D_{ji}^{(1)}, & j=k,\end{cases}\qquad D_{jk}^{(n)}=\begin{cases}2D_{jk}^{(n-1)}\left(D_{jj}^{(n-1)}-\dfrac{1}{x_j-x_k}\right), & j\neq k,\\ -\sum_{i\neq k}D_{ji}^{(n)}, & j=k.\end{cases}\tag{1.10}$$

As suggested in Theorem 3, the analytic region of u determines the convergence rate of its rational interpolation function. Therefore, conformal map g could be chosen to enlarge the ellipse of analyticity of $u\circ g$. Thus, a better approximation of u could be obtained. This is more accurate than using the Chebyshev spectral method with the same number of grid points.

Note that differentiation matrices (1.10) only rely on weights ω_k and new points $\hat{x}_k$, which is why the underlying equation does not need to be converted to new coordinates after mapping.

1.3. The* sinh*-transform. For solutions with a single boundary layer, Tee and Trefethen have constructed the conformal map [20]

$$g_{\lambda,\mu}(x)=\lambda+\mu\sinh\left[\left(\sinh^{-1}\left(\frac{1-\lambda}{\mu}\right)+\sinh^{-1}\left(\frac{1+\lambda}{\mu}\right)\right)\frac{x-1}{2}+\sinh^{-1}\left(\frac{1-\lambda}{\mu}\right)\right],\tag{1.11}$$

where $\lambda,\ \delta$ are the position and width of the boundary layers, respectively.

If $b>0,$ parameters in (1.11) should be chosen as

$$\lambda=1,\quad \delta=2T\varepsilon.$$

If there are two boundary layers, motivated by the work of Tee [20], we define the combined sinh-transform as:

$$\tilde{g}_\delta(x)=\begin{cases}\dfrac{1}{2}\left[g_{-1,\delta}(2x+1)-1\right], & x\in[-1,0),\\ \dfrac{1}{2}\left[g_{1,\delta}(2x-1)+1\right], & x\in[0,1].\end{cases}\tag{1.12}$$

If $b=0,$ the parameter in (1.12) should be chosen as $\delta=2\tau_0$.

2. Rational spectral collocation with the singularly separated method. By using the reaction-diffusion equation as an example, the implementation and error estimation of RSC-SSM are elaborated in this section.

2.1. The singularity-separated technique. Consider the problem (1.1) with $b = 0$. Homogenous equation $Lu = 0$ has two eigenvalues

$$\lambda_1 = \sqrt{\frac{c}{\varepsilon}}, \qquad \lambda_2 = -\sqrt{\frac{c}{\varepsilon}}.$$

Let u_0 be a special solution of $Lu = f$, its general solution is

$$u(x) = u_0(x) + C_1\phi_1(x) + C_2\phi_2(x), \quad \phi_1(x) = e^{\lambda_1(x-1)}, \quad \phi_2(x) = e^{\lambda_2 x}.$$

Note that if $\varepsilon = 10^{-k}$ and $k \geq 4$, $\phi_1(1) = \phi_2(0) = e^{\lambda_2} \approx e^{-1/\sqrt{\epsilon}} \approx 10^{-44} = 0$ can be neglect.

Thus, the solution $u(x)$ of the (1.1) can be decomposed into two parts, $u(x) = \omega(x) + v(x)$, in which $\omega(x) = u_0(x)$ is the regular term and $v(x) = C_1\phi_1(x) + C_2\phi_2(x)$ is the singular term. The regular term $\omega(x)$ is the solution of an auxiliary boundary-value problem

$$\begin{cases} L\omega = -\varepsilon\omega'' + c\omega = f(x), \\ \omega(0) = f(0)/c, \quad \omega(1) = f(1)/c. \end{cases} \tag{2.1}$$

Consequently, singular component $v(x)$ is given by

$$v(x) = C_1 e^{\lambda_1(x-1)} + C_2 e^{\lambda_2 x}.$$

Based on the boundary conditions, we obtain

$$C_2 = \alpha - \omega(0), \quad C_1 = \beta - \omega(1).$$

which satisfies $Lv = 0$. Then $v(0) = C_1 e^{-\lambda_1} \approx 0$ and $v(1) = C_2 e^{\lambda_2} \approx 0$.

2.2. RSC-SSM method. It is known from the boundary conditions of Eq. (2.1), that $\varepsilon\omega''(0) = \varepsilon\omega''(1) = 0$. The singularities of solution are weakened. The success of the new method is determined by the solution of the auxiliary equation (2.1). So, the rational spectral collocation with $\sinh$-transform would be chosen to solve Eq. (2.1).

First, by introducing the transform $x = 0.5(y + 1)$, $x \in [0, 1]$, $y \in [-1, 1]$ and defining $\hat{u}(y) = u(x) = u(0, 5(y + 1))$, then $u'(x) = 2\hat{u}'(y)$, $u''(x) = 4\hat{u}''(y)$, we can rewrite (2.1) as

$$\begin{cases} L\hat{\omega} = -4\varepsilon\hat{\omega}''(y) + c\hat{\omega}(y) = \hat{f}(y), & y \in (-1, 1), \\ \hat{\omega}(-1) = \hat{f}(-1)/c, & \hat{\omega}(1) = \hat{f}(1)/c. \end{cases} \tag{2.2}$$

The boundary layers are located at the two endpoints of $[-1, 1]$ and their width are $\delta = 2\tau_0$.

The transformed CGL collocation points are given

$$\{\hat{x}_k\}_{k=0}^N = \big\{g_\delta\big(-\cos(k\pi/N)\big)\big\}_{k=0}^N,$$

where the function g is shown in (1.12).

Calculating the equations in (1.12) at points $\{\hat{x}_k\}_{k=0}^{N}$ yields

$$4\varepsilon D^{(2)}\hat{W} + c\hat{W} = \hat{F}. \tag{2.3}$$

The boundary conditions in (1.12) suggest that

$$\hat{W}(1) = \hat{f}(1)/c, \quad 2b\hat{W}(N+1) = \hat{f}(N+1)/c. \tag{2.4}$$

In operator form the governing equation (2.3) becomes

$$A\hat{W} = \hat{F}, \tag{2.5}$$

where $A = 4\varepsilon D^{(2)} + cE_{N+1}$.

The first end last rows of the matrix A are replaced with $e_1 = (1, 0, \ldots, 0)$, $e_{N+1} = = (0, \ldots, 0, 1)$, respectively. Solving the linear algebra system including (2.4) and (2.5), we get the numerical solution of (2.1).

According to the boundary condition of the original problem (1.1) and the value of the regular component, the parameters of singular terms are obtained.

By using this method, the following numerical solution of Eq. (1.1) can be received

$$u_{ss}(x) = \omega(x) + v(x).$$

2.3. Error analysis. The following stability results about $u(x)$ and $u'(x)$ were given in [16].

Theorem 4. *The solution for the problem $u(x)$ has the estimates*

$$|u(x)| \le M = \max(|u_0|, |u_1|) + C \max |f(x)|,$$

$$|u'(x)| \le CM/\varepsilon.$$

Theorem 5. *The numerical solution u_{ss} convergences to the exact solution u of the problem (1.1) and satisfies the following error estimates:*

$$\|u(x) - u_{ss}(x)\| \le Me^{-\sqrt{c/\varepsilon}}, \qquad \left\|u'(x) - u'_{ss}(x)\right\| \le M\,\frac{|v(0)|}{\varepsilon}. \tag{2.6}$$

Proof. Let $z = u - u_{ss}$. Then z satisfies

$$Lz = L(u(x) - u_{ss}(x)) = Lu(x) - L\omega(x) - Lv(x) = 0, \quad x \in (0, 1),$$

and

$$\|(u - u_{ss})(0)\| = \|u(0) - \omega(0) - C_1 e^{-\sqrt{\frac{c}{\varepsilon}}} - C_2\| = \|C_1\| e^{-\sqrt{\frac{c}{\varepsilon}}},$$

$$\|(u - u_{ss})(1)\| = \|u(1) - \omega(1) - C_1 - C_2 e^{-\sqrt{\frac{c}{\varepsilon}}}\| = \|C_2\| e^{-\sqrt{\frac{c}{\varepsilon}}}.$$

According to Theorem 4, the conclusion is established.

3. Numerical experiments. In order to verify the accuracy and efficiency of our method, the RSCAT method and RSC-SSM are used to solve the problems with exact solutions and compare the results. The theoretical results obtained in the previous section are verified through numerical experiments. The maximum relative errors of the solution are given by

$$e = \frac{\|u_N - u\|_\infty}{\|u_E\|_\infty},$$

where $u_N,\ u$ are the numerical solution and the exact solution, respectively.

In our computations, all experiments are performed by using MATLAB (version R2014a) on a personal computer with a 2.5-Hz central processing unit (Intel Core i5-2450M), 4.00 GB of memory and Windows 7 operating system.

Example 1. Consider the nonhomogeneous convection-diffusion singular perturbation problem $c = 0$ [21] (example 2)

$$\varepsilon y'' + y' = 1 + 2x, \quad 0 < x < 1, \quad y(0) = 0, \quad y(1) = 1. \tag{3.1}$$

This problem has rapid chances near the point $x = 0,$ and the width of boundary layer is $\delta = \varepsilon \ln \frac{1}{\varepsilon}$. The exact solution of (3.1) is given as

$$y(x) = x^2 + (1 - 2\varepsilon)x + \frac{2\varepsilon - 1}{1 - e^{-1/\varepsilon}} \left(1 - e^{-\frac{x}{\varepsilon}}\right). \tag{3.2}$$

By using singularly separated technology, the auxiliary boundary-value problem is as follows:

$$\begin{cases} \varepsilon y'' + y' = 1 + 2x, & 0 < x < 1, \\ y'(0) = 1, & y(1) = 1. \end{cases}$$

The singular term can be expressed as

$$v(x) = C_1 e^{\lambda_1 x},$$

where $\lambda_1 = -\frac{1}{\varepsilon}$ is one of the eigenvalue with ε.

Figure 1 plots the maximum relative errors of both RSC-SSM and RSCAT method in semi-log scale for various values of ε. Compared with RSCAT method, the rates of convergence are considerably improved in our RSC-SSM. Furthermore, the numerical results of the RSC-SSM and RSCAT method are compared in Table 1. We observe that our method offers better results with fewer unknowns. RSC-SSM takes less time for the same number of unknowns.

The plots of numerical and exact solutions with various values of ε are displayed in Fig. 2. The pointwise errors of this problem is shown in Fig. 3. We see that the errors are almost constant for each point with the various values of ε. Because there is a reasonably high number of collocation points in the boundary layer region, the behavior of the boundary layer region is well characterized.

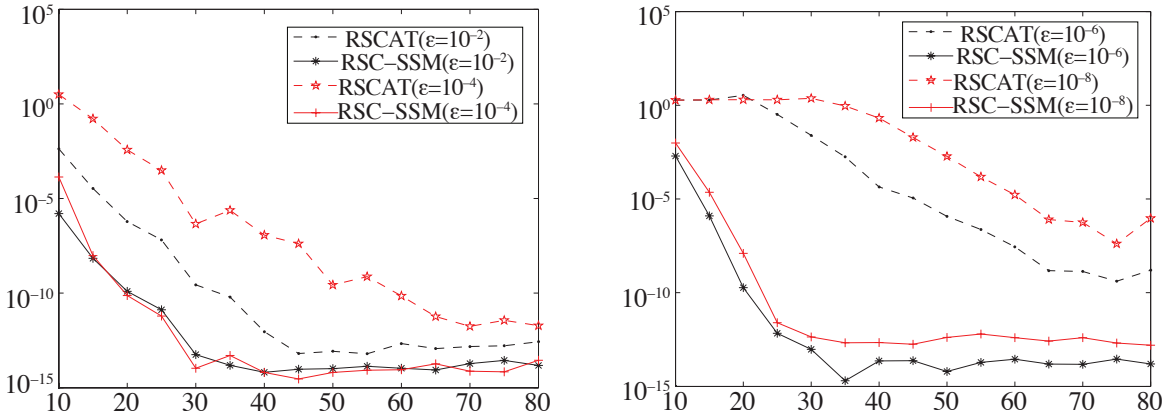

Fig. 1. Relative errors in Example 1: RSCAT method (dashed lines) vs. RSC-SSM method (solid lines).

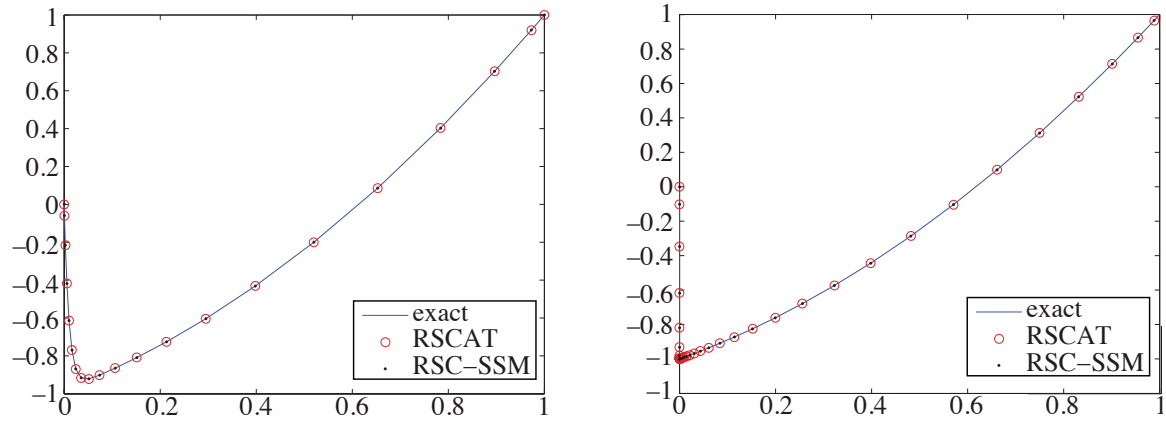

(a) $\varepsilon = 10^{-2}$, $N = 20$ *(b)* $\varepsilon = 10^{-8}$, $N = 80$

Fig. 2. Numerical solutions vs. exact solutions. RSCAT (dashes lines) vs. RSC-SSM method (solid lines).

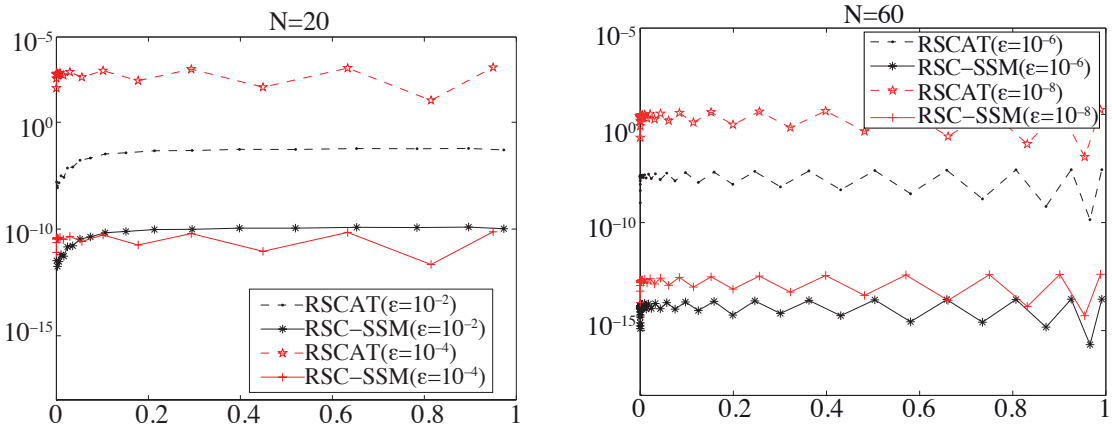

Fig. 3. Point wise errors. RSCAT(dashes lines) vs. RSC-SSM method (solid lines).

Table 1. Calculation results of maximum relative error and CPU time for Example 4.1

ε	N	RSC-SSM		RSCAT		Save time %
		e_1	t	e_1	t	
1e-2	20	6.03e-07	0.0013	1.23e-10	0.0011	15.38
1e-4	40	1.16e-07	0.0015	6.44e-15	0.0014	6.67
1e-6	60	2.81e-08	0.0034	2.81e-14	0.0021	38.24
1e-8	90	1.05e-06	0.0027	1.98e-13	0.0016	29.73

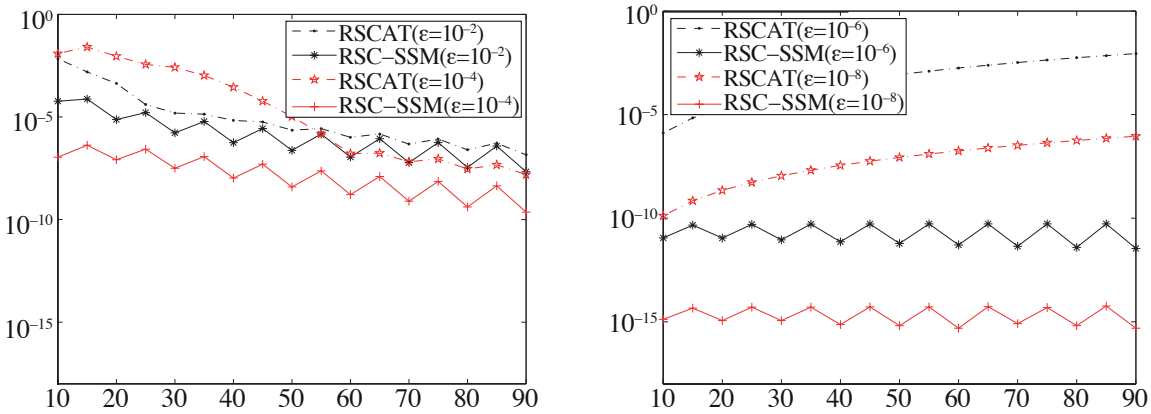

Fig. 4. Relative errors in Example 2: RSCAT method (dashed lines) vs. RSC-SSM method (solid lines).

Example 2. When $b = 0$, consider the reaction-diffusion problem.

$$-\varepsilon^2 y'' + y = e^x, \quad 0 < x < 1, \quad y(0) = 0, \quad y(1) = 0. \tag{3.3}$$

The exact solution can be expressed as

$$y(x) = \frac{e^{-x/\varepsilon}\left(e^{1-1/\varepsilon} - 1\right) + e^{-(1-x)/\varepsilon}\left(e^{1/\varepsilon} - e\right)}{(1-\varepsilon^2)\left(1 - e^{-2/\varepsilon}\right)} + \frac{e^x}{1-\varepsilon^2}.$$

This problem has two boundary layer regions, i.e., the location of boundary layer are the two endpoints of the underlying interval $[0, 1]$. The two eigenvalues of this problem are $\lambda_1 = -1/\varepsilon$, $\lambda_2 = 1/\varepsilon$. Therefore, the singular term can be expressed

$$v(x) = C_1 e^{\lambda_1 x} + C_2 e^{\lambda_2 (x-1)}.$$

The auxiliary boundary-value problem of (3.3) is as follows:

$$\begin{cases} -\varepsilon^2 y'' + y = e^x, & 0 < x < 1, \\ y(0) = 1, & y(1) = e. \end{cases}$$

The maximum relative errors between RSC-SSM and RSCAT method are compared in Fig. 4 and Table 2, which verify the high accuracy and efficiency of RSC-SSM. Furthermore, displays the plots of solutions and the pointwise errors with various values of and N are given in Fig. 5 and Fig. 6, respectively.

Table 2. Comparison of the relative maximum errors and CPU time of Example 4.2

ε	N	RSC-SSM		RSCAT		Save time %
		e_1	t	e_1	t	
1e-2	20	4.28e-04	0.0013	7.49e-6	0.0010	23.08
1e-4	40	2.82e-04	0.0027	1.06e-8	0.0017	37.04
1e-6	80	5.57e-03	0.0031	9.02e-13	0.0024	25.58
1e-8	90	9.01e-07	0.0087	4.90e-16	0.0023	73.56

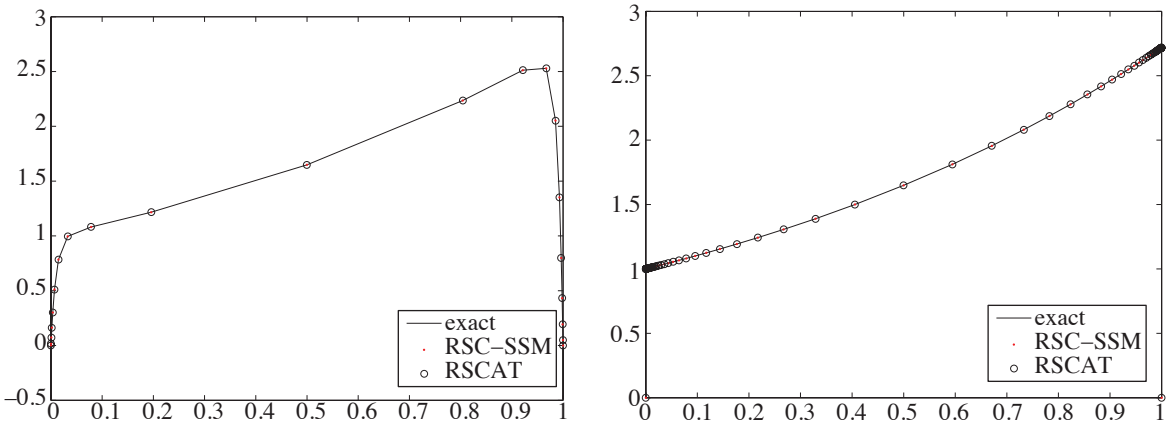

(a) $\varepsilon = 10^{-2}$, $N = 20$ *(b)* $\varepsilon = 10^{-8}$, $N = 90$

Fig. 5. Numerical solutions vs. exact solutions. RSCAT (dashes lines) vs. RSC-SSM method (solid lines).

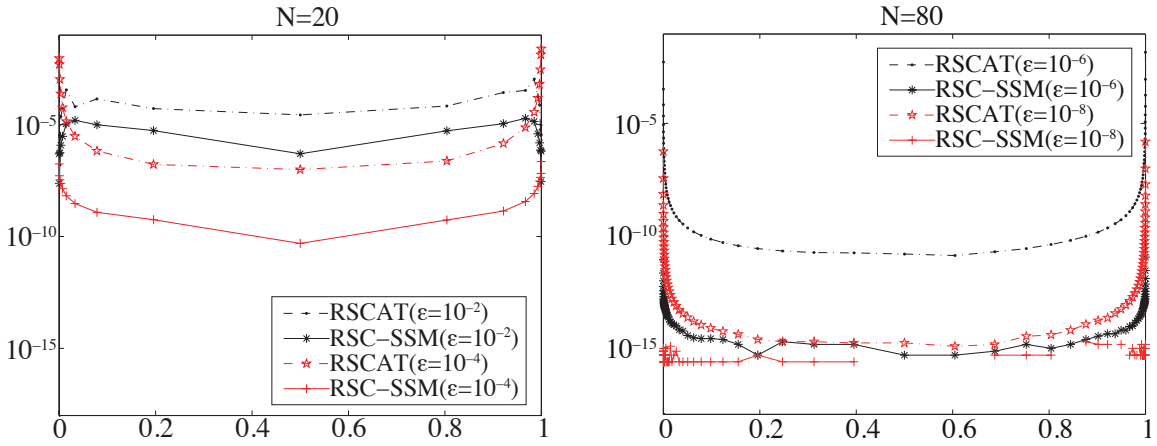

Fig. 6. Point wise errors. RSCAT (dashes lines) vs. RSC-SSM method (solid lines).

Additionally, Fig. 5 displays the plots of numerical and exact solutions with $\varepsilon = 10^{-2}, 10^{-8}$ in the whole region. The point-wise errors of the function with different ε and N are given in Fig. 6.

4. Conclusion. A novel numerical method named RSC-SSM, has been proposed to solve a class of second-order singularly perturbed boundary-value problems in this paper. The solution is composed of a weaker singularity auxiliary solution and a singular correct function. Numerical experiments confirm that, compared to RSCAT, RSC-SSM has the following advantages:

1. The new method solves an auxiliary weak singular boundary-value problem instead of the original problem. The weaker singularity reduces the impact of perturbation parameters on the problem and improves the accuracy of the solution.

2. The parameters in the singular term can be determined by the boundary conditions and regular terms of the original problem (i.e., the singular term has an explicit expression).

3. The accuracy of numerical approximation depends not only on the number of the grid nodes, but also on the parameter ε. The smaller ε is, the thinner the boundary layer is, and the better results can be obtained.

The numerical results demonstrate the spectral accuracy of the proposed algorithm and agree with the theoretical analysis. Moreover, the numerical method and theoretical results presented in this paper can be extended to more complex problems.

References

1. M. K. Kadalbajoo, K. C. Patidar, *A survey of numerical techniques for solving singularly perturbed ordinary differential equations*, Appl. Math. Comput., **130**, 223 – 259 (2002).

2. M. Kumar, N. Singh, *A collection of computational techniques for solving singular boundary-value problems*, Adv. Eng. Softw., **40**, 288 – 297 (2010).

3. M. K. Kadalbajoo, V. Gupta, *A brief survey on numerical methods for solving singularly perturbed problems*, Appl. Math. Comput., **217**, № 8, 3641 – 3716 (2010).

4. P. A. Lagerstrom, *Matched asymptotic expansions: ideas and techniques*, Appl. Math. Sci., **76**, Springer-Verlag, New York (1988).

5. A. M. Wazwaz, F. B. Hanson, *Matched uniform approximations for a singular boundary and interior turning point*, SIAM J. Appl. Math., **46**, № 6, 943 – 961 (1986).

6. M. Nakano, *Second-order linear ordinary differential equations with turning points and singularities. I*, Kōdai Math. Sem. Rep., **29**, № 1-2, 88 – 102 (1977).

7. M. Nakano, *Second-order linear ordinary differential equations with turning points and singularities. II*, Kōdai Math. J., **1**, № 2, 304 – 312 (1978).

8. J. J. H. Miller, E. O'Riordan, G. I. Shishkin, *Fitted numerical methods for singular perturbation problems. Error estimates in the maximum norm for linear problems in one and two dimensions*, World Sci. Publ. Co., Inc., River Edge, NJ (1996).

9. N. Madden, M. Stynes, *A uniformly convergent numerical method for a coupled system of two singularly perturbed linear reaction-diffusion problems*, IMA J. Numer. Anal., **23**, 627 – 644 (2003).

10. T. Linß, N. Madden, *An improved error estimate for a numerical method for a system of coupled singluar perturbed reaction-diffusion equations*, Comput. Methods Appl. Math., **3**, 417 – 423 (2003).

11. A. Tariq, K. Arshad, *A spline method for second-order singularly perturbed boundary-value problems*, Comput. Appl. Math., **42**, 445 – 452 (2002).

12. R. Baltensperger, J. P. Berrut, Y. Dubey, *The linear rational pseudospectral method with preassigned poles*, Numer. Algorithms, **33**, 53 – 63 (2003).

13. J. P. Berrut, R. Baltensperger, H. D. Mittelmann, *Recent development in barycentric rational interpolation, Trends and Applications in Constructive Approximation*, Internat. Ser. Numer. Math., **151**, Birkhäuser, Basel, 27 – 51 (2005).

14. S. Chen, Yi. Wang, *A rational spectral collocation method for third-order singularly perturbed problems*, J. Comp. Appl. Math., **307**, 93 – 105 (2016).

15. S. Chen, Yi. Wang, and X. Wu, *Rational spectral collocation method for a coupled system of singularly perturbed boundary valus problems*, J. Comput. Math., **29**, № 4, 458 – 473 (2011).

16. Ch. Chen, J. Yang, *The singularity-separated method for the singular perturbation problems in 1-D*, Int. J. Numer. Anal. Model., **15**, № 1-2, 102 – 110 (2017).

17. E. M. de Jager, Furu Jiang, *The theory of singular pertubations*, North-Holland Ser. Appl. Math. Mech., **42**, North-Holland Publ. Co., Amsterdam (1996).

18. J. P. Berrut, L. N. Trefethen, *Barycentric Lagrange interpolation*, SIAM Rev., **46**, № 3, 501 – 517 (2004).

19. Richard Baltensperger, Jean-Paul Berrut, Benjamin Noël, *Exponential convergence of a linear rational interpolant between transformed Chebyshev points*, Math. Comput., **68**, 1109 – 1120 (1999).

20. T. W. Tee, Lloyd N. Trefethen, *A rational spectral collocation method with adaptively transformed Chebyshev grid points*, SIAM J. Sci. Comput., **28**, № 5, 1798 – 1811 (2006).

21. Awoke Andargie, *Fourth order fitted scheme for second order singular perturbation boundary-value problems*, Amer. J. Comput. Appl. Math., **2**, № 1, 25 – 29 (2012).

Received 12.01.19